JOURNAL OF THE AMERICAN COLLEGE OF CARDIOLOGY
© 2015 BY THE AMERICAN COLLEGE OF CARDIOLOGY FOUNDATION
PUBLISHED BY ELSEVIER INC.

VOL. 65, NO. 14, 2015
ISSN 0735-1097/$36.00
http://dx.doi.org/10.1016/j.jacc.2015.01.045

Exercise Triggers ARVC Phenotype in Mice Expressing a Disease-Causing Mutated Version of Human Plakophilin-2

Francisco M. Cruz, PhD,* David Sanz-Rosa, PhD,† Marta Roche-Molina, PhD,* Jaime García-Prieto, BSc,† José M. García-Ruiz, MD,† Gonzalo Pizarro, MD,† Luis J. Jiménez-Borreguero, MD,† Miguel Torres, PhD,* Antonio Bernad, PhD,* Jesús Ruíz-Cabello, PhD,‡ Valentín Fuster, MD, PhD,†§ Borja Ibáñez, MD, PhD,†‖ Juan A. Bernal, PhD*

ABSTRACT

BACKGROUND Exercise has been proposed as a trigger for arrhythmogenic right ventricular cardiomyopathy (ARVC) phenotype manifestation; however, research is hampered by the limited availability of animal models in which disease-associated mutations can be tested.

OBJECTIVES This study evaluated the impact of exercise on ARVC cardiac manifestations in mice after adeno-associated virus (AAV)–mediated gene delivery of mutant human *PKP2*, which encodes the desmosomal protein plakophilin-2.

METHODS We developed a new model of cardiac tissue-specific transgenic-like mice on the basis of AAV gene transfer to test the potential of a combination of a human *PKP2* mutation and endurance training to trigger an ARVC-like phenotype.

RESULTS Stable cardiac expression of mutant *PKP2* (c.2203C>T), encoding the R735X mutant protein, was achieved 4 weeks after a single AAV9-R735X intravenous injection. High-field cardiac magnetic resonance over a 10-month postinfection follow-up did not detect an overt right ventricular (RV) phenotype in nonexercised (sedentary) mice. In contrast, endurance exercise training (initiated 2 weeks after AAV9-R735X injection) resulted in clear RV dysfunction that resembled the ARVC phenotype (impaired global RV systolic function and RV regional wall motion abnormalities on cardiac magnetic resonance). At the histological level, RV samples from endurance-trained R735X-infected mice displayed connexin 43 delocalization at intercardiomyocyte gap junctions, a change not observed in sedentary mice.

CONCLUSIONS The introduction of the *PKP2* R735X mutation into mice resulted in an exercise-dependent ARVC phenotype. The R735X mutation appears to function as a dominant-negative variant. This novel system for AAV-mediated introduction of a mutation into wild-type mice has broad potential for study of the implication of diverse mutations in complex cardiomyopathies. (J Am Coll Cardiol 2015;65:1438–50) © 2015 by the American College of Cardiology Foundation.

From the *Cardiovascular Development and Repair Department, Centro Nacional de Investigaciones Cardiovasculares, Madrid, Spain; †Epidemiology, Atherothrombosis and Imaging Department, Centro Nacional de Investigaciones Cardiovasculares, Madrid, Spain; ‡Advanced Imaging Unit, Epidemiology, Atherothrombosis and Imaging Department, Ciber de Enfermedades Respiratorias and Universidad Complutense, Madrid, Spain; §The Zena and Michael A. Wiener Cardiovascular Institute, Mount Sinai School of Medicine, New York, New York; and the ‖Cardiovascular Institute, Hospital Clínico San Carlos, Madrid, Spain. This study was supported by grants from the Spanish Ministry of Economy and Competitiveness and the "Fondo de Investigacion Sanitaria" (BFU2012-35258 grant to Dr. Bernal, Ramón y Cajal Program grant RYC-2009-04341 to Dr. Bernal, and FIS10/02268 to Dr. Ibáñez), and fellowship FPU-AP2010-5951 to Dr. Cruz. The Centro Nacional de Investigaciones Cardiovasculares Carlos III (CNIC) is supported by the Ministerio de Economia y Competitividad (MINECO) and the Pro-CNIC Foundation. The authors have reported that they have no relationships relevant to the contents of this paper to disclose. Hugh Calkins, MD, served as Guest Editor for this article.
Listen to this manuscript's audio summary by *JACC* Editor-in-Chief Dr. Valentin Fuster.
You can also listen to this issue's audio summary by *JACC* Editor-in-Chief Dr. Valentin Fuster.

Manuscript received October 1, 2014; revised manuscript received January 27, 2015, accepted January 29, 2015.

Arrhythmogenic right ventricular cardiomyopathy (ARVC) is a heart muscle disease, clinically characterized by right ventricular (RV) anatomic abnormalities and an above-normal incidence of ventricular arrhythmia that can lead to sudden cardiac death, especially in young people. Many cases involve a familial association, and several mutations have been identified (1,2).

SEE PAGE 1451

ARVC onset is unpredictable; a gene-environment interaction has been suggested to trigger the disease's anatomic/electrical development, but this proposal is still deliberated. Ventricular arrhythmias and sudden death have been linked to exercise, which led to the recommendation that patients carrying an ARVC-causing mutation withdraw from endurance exercise (3); however, the effect of exercise on the onset and development of the anatomic ARVC phenotype is strongly debated.

In most cases, ARVC first manifests, after an initial concealed phase, as areas of RV dyskinesis that develop into isolated right-sided heart dysfunction and finally biventricular failure and fibrofatty replacement of heart muscle (4). Beyond reducing the incidence of arrhythmias with antiarrhythmic drugs or an implantable cardioverter-defibrillator, no treatment can effectively prevent disease progression.

ARVC is a paradigm of a complex cardiomyopathy caused by an autosomal dominant trait (5,6). Of the 8 genes linked to ARVC (7), 5 encode desmosomal proteins and account for ~50% of ARVC probands (5). The more than 380 mutations identified in ARVC patients include 161 pathogenic variants of *PKP2*, which encodes the desmosomal protein plakophilin-2. In several series, the prevalence of *PKP2* mutations in ARVC patients was >40% (8,9). Despite the strong implication of *PKP2* mutations in ARVC, there are no available transgenic disease models that express *PKP2* mutant alleles (10).

To study the effect of exercise on hearts of mice carrying the most prevalent ARVC-associated mutation (*PKP2*), we used adeno-associated virus (AAV)-mediated *PKP2* mutant gene transfer to express an ARVC-causing mutation in the cardiomyocytes of wild-type mice. After stable expression of mutant *PKP2*, we studied RV function by high-field cardiac magnetic resonance (CMR) in sedentary and endurance-trained mice.

METHODS

Four- to 6-week-old wild-type C57BL6/J mice were injected with 3.5×10^{10} viral genomes encoding luciferase (*Luc*), wild-type human *PKP2*, or the C-terminal deletion mutant version, R735X. Animals were divided into group A (trained) and group B (sedentary). Training in group A started 2 weeks after injection and continued for 8 consecutive weeks. At the end of that period, *Luc*, *PKP2*, and R735X mice were imaged by CMR and euthanized for heart sampling. Animals in group B were analyzed by CMR 6 and 10 months after infection with AAV particles.

All CMR images were analyzed with dedicated software (QMass MR version 7.5, Medis, Leiden, the Netherlands) by 2 experienced observers blinded to the study allocation. All CMR images were of good quality and could be analyzed. The short-axis dataset was analyzed quantitatively by manual detection of endocardial borders in end diastole and end systole with exclusion of papillary muscles and trabeculae to obtain both left and right end-diastolic volume, end-systolic volume, and ejection fraction (EF). Wall motion was classified as abnormal in the presence of akinesia, dyskinesia (in ventricular systole), or bulging (in ventricular diastole).

Experiments used the minimum number of mice needed to give sufficient statistical power, and no animals were excluded from the analyses. Data were analyzed by 1-way analysis of variance, 2-way analysis of variance, and Student *t* test. Relative risk analysis was assessed by 2-tailed Fisher exact test. CMR measure reliability was assessed by interobserver intraclass correlation coefficient (absolute agreement) and mean bias.

Additional materials and methods are available in the Online Appendix.

RESULTS

We generated enhanced green fluorescence protein (EGFP)-reporter AAV vectors driven from the cardiomyocyte-specific cardiac troponin T proximal promoter and encoding Luc, wild-type human PKP2a (the major splice variant in the heart), or a C-terminal deletion PKP2a mutant (R735X) (**Figures 1A and 1B**). We chose the R735X mutation because exon 11 is a hot spot for mutations that give rise to truncated PKP2 products found in ARVC patients (11–13) (**Figure 1C**). To further test whether genetic haploinsufficiency operates after expression in trans of R735X mutant, we measured the endogenous mouse *Pkp2* transcript level. In AAV-R735X transduced mice, endogenous *Pkp2* messenger ribonucleic acid (mRNA) levels remained stable (**Figure 1D**), which demonstrates that

ABBREVIATIONS AND ACRONYMS

AAV = adeno-associated virus

ARVC = arrhythmogenic right ventricular cardiomyopathy

CMR = cardiac magnetic resonance

Cx43 = connexin 43

EF = ejection fraction

EGFP = enhanced green fluorescence protein

Luc = luciferase

LV = left ventricle

mRNA = messenger ribonucleic acid

PKP2 = plakophilin-2

R735X = C-terminal deletion PKP2a mutant

RV = right ventricle

FIGURE 1 AAV Construct to Express Transgenes in Cardiomyocytes

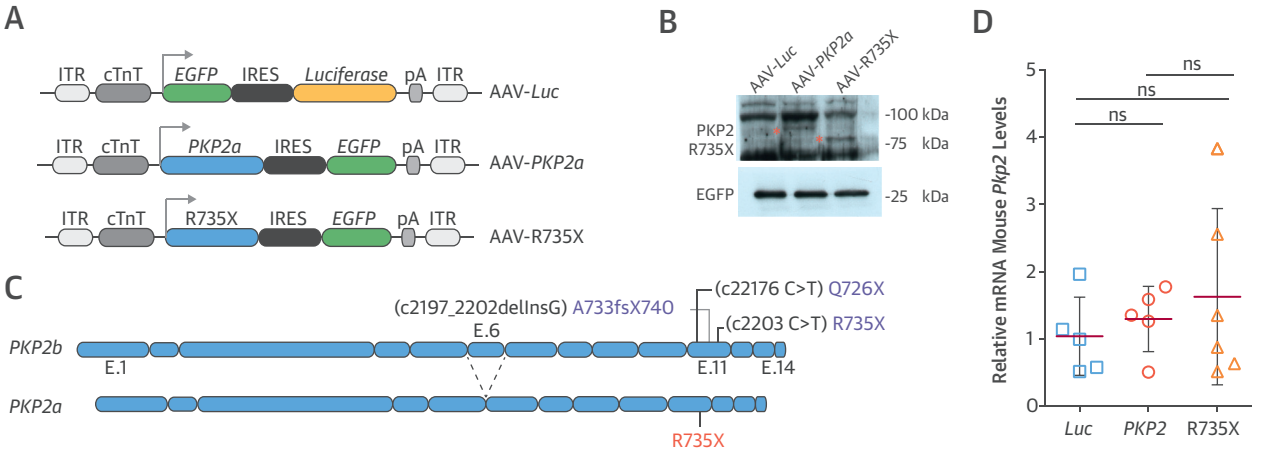

(A) Adeno-associated virus (AAV) vectors encoding human wild-type PKP2a or the R735X mutant variant driven by the cardiac troponin T (cTnT) proximal promoter and followed by enhanced green fluorescence protein (EGFP) after an internal ribosome entry site (IRES). In the control luciferase (*Luc*) vector, EGFP is placed after the cTnT proximal promoter, and the Luc follows the IRES. AAV inverted terminal repeats (ITR) and the poly-adenylation sequence (pA) are also indicated. **(B)** Western blot shows cardiac expression of PKP2a, R735X, and EGFP. Red asterisk indicates proteins encoded by the transgene. **(C)** Alignment of alternatively spliced versions of human PKP2. Exon 6 is missing in the PKP2a cardiac isoform. Nonsense mutations in PKP2b exon 11 associated with ARVC are indicated in blue (c.2176C>T, Q726X; c.2197_2202delinsG, A733fsX740; c.2203C>T, R735X); the equivalent mutant in PKP2a (R735X) used in this study is indicated in red. **(D)** Quantitative polymerase chain reaction of hearts infected with AAV expressing *Luc*, *PKP2*, and R735X showing stable *Pkp2* endogenous levels. mRNA = messenger ribonucleic acid; PKP2 = plakophilin-2.

mutant R735X transcript does not induce degradation of mouse *Pkp2* messenger.

Cardiac expression was potentiated by packaging the vector in the AAV9 capsid serotype, the most efficient envelope protein for cardiomyocyte gene delivery in mice (14). Viral particles (3.5×10^{10} per animal) were administered to 4- to 5-week-old mice through the intravenous femoral route. Two weeks after injection, in vivo bioluminescence signal was evident in all injected Luc control mice, reaching a plateau after 4 weeks (**Figure 2A**). Ex vivo bioluminescence imaging of organs from these mice showed that signal was present in liver and more intensely in heart (**Figure 2B**). Subsequent quantitative polymerase chain reaction quantification of *PKP2* and *EGFP* mRNA confirmed this expression pattern (Online Figure 1), showing 40-fold higher expression of these genes in heart than in liver. AAV9-mediated delivery of a gene driven from a cardiac-specific cardiac troponin T promoter thus preferentially produces activity in the heart after systemic intravenous administration. Further analysis demonstrated a mosaic distribution of transgene expression throughout the heart, which corresponded to a cardiomyocyte transduction rate (quantified by EGFP immunofluorescence) of 95 ± 2% (**Figure 2C**). Analysis by *k*-means clustering for segmented images showed that cell fluorescence intensities clustered around integer values, with >50% of cardiomyocytes having a signal intensity that corresponded to a viral genome number between 1 and 3 (**Figure 2D**). These data confirm that AAV infection occurs throughout the heart and that cardiomyocytes stably express the specific targeted transgenes.

To assess the effect of transgene expression on cardiac phenotype, we evaluated typical anatomic features of ARVC in sedentary animals by high-field (7 Tesla) CMR at 10 months after AAV infection. After quantitative (RV end-diastolic volume, end-systolic volume, and EF) and qualitative (RV wall motion abnormalities) analyses, we did not find any sign of RV dysfunction in sedentary mice (**Figures 3A** [left panel], **3B, and 3C**), despite long-term expression of transgenes in cardiomyocytes (Online Figure 2). In addition, surface electrocardiographic analysis revealed that QRS duration in AAV-R735X mice was prolonged compared with control mice that expressed wild-type PKP2 or Luc (Online Figure 3A).

Exercise training has been proposed to accelerate the appearance of ARVC disease features in humans (15,16) and in a plakoglobin-haploinsufficient animal model (17), although this association has not been demonstrated formally when expressing a potential

FIGURE 2 **AAV-Mediated Gene Distribution in Mouse Hearts**

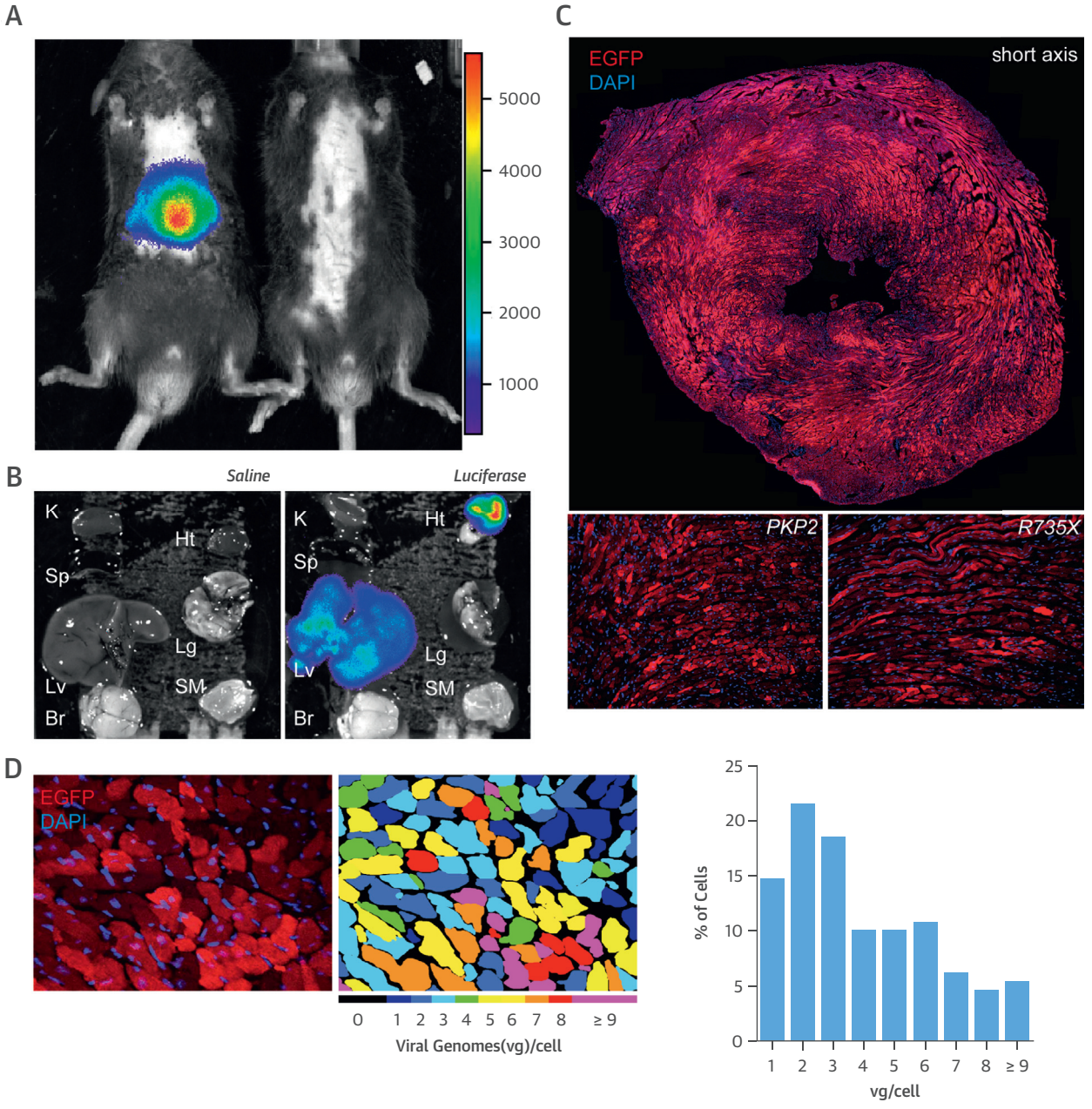

(A) Representative live-animal bioluminescence imaging of luciferase (Luc) transgene expression in a C57BL6J mouse injected intravenously (femoral vein) with AAV2-based vector in packaging serotype 9 (dose 3.5 × 1,010 viral genomes [vg] in 50 μl of saline solution), shown next to a mock-injected mouse (saline solution). Bioluminescence images were acquired 4 weeks after inoculation. **(B)** Ex vivo bioluminescence images from explanted organs of a mouse injected with the Luc-based vector (Br = brain; Ht = heart; K = kidney; Lg = lung; Lv = liver; SM = skeletal muscle; and Sp = Spleen). Luc activity was predominant in the heart with a weaker bioluminescent signal in liver. **(C)** Representative fluorescence microscopy images of short-axis cross sections of AAV-transduced hearts illustrate expression of EGFP throughout the heart. Magnified images show the mosaic cellular distribution of wild-type PKP2 and R735X expression in the heart. **(D)** Fluorescence intensity quantification of transduced protein expression, used to assign the number of integrated viral genomes per cardiomyocyte. Other abbreviations as in Figure 1.

FIGURE 3 Anatomic CMR Analysis After AAV Infection

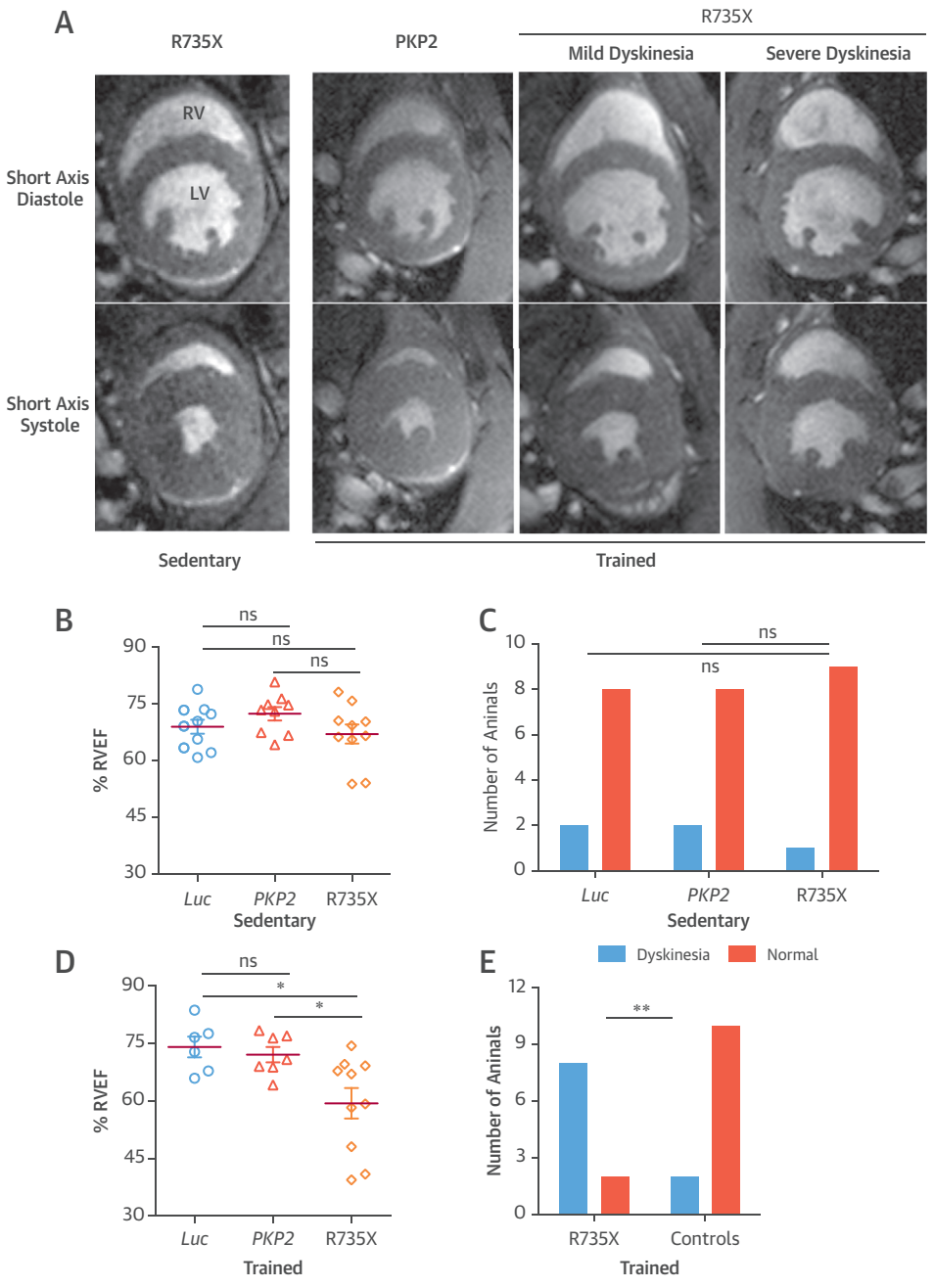

(A) Representative short-axis cardiac magnetic resonance (CMR) images taken at the end of diastole and systole in mice transduced with wild-type PKP2 or the R735X mutant. The left panels show representative images of a normal heart from a 10-month-old sedentary animal transduced with AAV-R735X. Right panels show CMR images from mice infected with PKP2 or R735X virus and subjected to 8 weeks of endurance training (RV = right ventricle; LV = left ventricle). **(B)** Percent RV ejection fraction (% RVEF) in hearts of 10-month-old sedentary mice transduced with the Luc, PKP2, or R735X AAV vectors. **(C)** Incidence and relative risk of dyskinetic events in the RV wall of R735X, Luc, and PKP2-transduced mice. **(D)** Analysis as in **(B)** for 8-week exercise-trained mice; *$p < 0.05$. **(E)** Analysis as in **(C)** in exercise-trained R735X-transduced mice and control animals (relative risk: 4.8). **$p = 0.008$ (2-tailed Fisher exact test). Online Videos 1, 2, and 3 contain CMR cines showing RV contractility. Abbreviations as in **Figure 1**.

dominant-negative mutant. To test this hypothesis in our disease model, we subjected mice to an 8-week swimming endurance training protocol, starting 2 weeks after AAV9 injection and cardiac *trans*-expression of *Luc*, wild-type *PKP2*, or mutant *PKP2*-R735X. To evaluate the ARVC phenotype in trained animals, we specifically quantified typical anatomic disease features by high-field (7 T) CMR after 8 weeks of training (**Figure 3A**, right panels). These functional imaging studies revealed quantitative and qualitative RV abnormalities in mice carrying the R735X mutation after training (**Figures 3D and 3E**) (Online Videos 1, 2, and 3).

RV EF in these mice (59.3 ± 3.9%; n = 10) was lower than in mice expressing wild-type *PKP2* (72.4 ± 1.9%; n = 6) or *Luc* (74 ± 2.7%; n = 7; $p < 0.05$) (**Figure 3D**). Contrary to trained mice, sedentary animals analyzed at 6 and 10 months after infection showed normal RV EF (n = 10; 68.9 ± 1.8%, 72.4 ± 1.9%, and 67 ± 2.5% in *Luc*, wild-type *PKP2*, and R735X mutant respectively; p = NS) (**Figure 3B**, after 10 months), which indicates a direct relationship between exercise and ventricular dysfunction. Interobserver intraclass correlation coefficient (absolute agreement) and mean bias of EF CMR measures were 0.91 (95% confidence interval: 0.78 to 0.96) and 0.9 μl (95% confidence interval: −0.6 to 2.4), respectively.

Evaluation of regional RV wall motion revealed areas of poor contractility, a specific characteristic of ARVC (4), in animals carrying the R735X mutation only when subjected to endurance training. The RV was divided into 11 segments (18). Wall motion was classified as abnormal in the presence of akinesia, hypokinesia, dyskinesia (in ventricular systole), or bulging (in ventricular diastole). Dichotomic diagnosis of ARVC by pre-specified dyskinetic analysis of these events identified the disease in 8 of 10 mice expressing the R735X mutant form of *PKP2,* compared with just 2 of 13 control mice (1 of 7 and 1 of 6 expressing wild-type *PKP2* or *Luc*, respectively; p = 0.008) (**Figure 3D**). In sedentary mice, dyskinetic events occurred less frequently and did not correlate with any genotype after 10 months (1 of 10, 2 of 10, and 2 of 10 expressing the R735X mutant, wild-type *PKP2*, or *Luc*, respectively; p = 0.78) (**Figure 3C**). The CMR analysis thus confirmed that AAV-mediated cardiac trans-expression of a disease-associated *PKP2* mutation in mice generates a phenotype characteristic of ARVC only after endurance training. Surface electrocardiographic analysis in trained mice revealed a trend toward QRS prolongation in animals expressing R735X mutant compared with control mice expressing wild-type *PKP2* or *Luc* (Online Figure 3B).

The advanced stages of ARVC are usually associated with fibrofatty replacement of RV ventricular mass (19). Despite the clear ARVC anatomic phenotype of endurance-trained R735X-infected mice in the imaging analysis, post-mortem histological evaluation revealed no evidence of myocardial fibrosis or fibrofatty cardiomyocyte replacement. Similarly, sedentary AAV-R735X–infected animals showed no evidence of fibrosis on post-mortem histological analysis at 6 months after infection. An absence of RV fibrofatty replacement was also reported in humans and plakoglobin-haploinsufficient mice, in which structural abnormalities in the RV were not linked to lipidic or fibrotic tissue infiltration (17). This particular *PKP2* dominant-negative model thus provides a complementary example of a mutant that segregates late cellular replacement events historically linked to the disease from the CMR-defined RV dysfunction used for clinical diagnosis.

ARVC is often considered a desmosomal protein disease (20) because of its association with mutations in the genes encoding the 5 desmosomal protein components (Online Figure 4); however, patient biopsy samples and transgenic mouse models of ARVC do not always show evidence of ultrastructural abnormalities in cell-to-cell junctions (17,21). Transmission electron microscopy of heart tissue from exercised R735X-infected mice revealed normal desmosome organization and uniform intercellular spacing (**Figures 4A and 4B**). Plakoglobin signal level in heart biopsy samples has been suggested as a potential marker of ARVC (22). Immunocytochemical analysis of desmosome revealed proper plakoglobin localization between the cardiomyocytes in all mice injected (**Figure 4C**), similar to what could be observed when samples were stained for PKP2 (**Figure 4D**). However, R735X-infected hearts did show alterations in the localization and distribution of the principal gap-junction component connexin 43 (Cx43) (23) at the short ends of cardiomyocytes (**Figure 5A**), despite normal expression levels of Cx43 mRNA and protein (Online Figures 5A and 5B). Cx43 gap junctions are required for proper electrical coupling between neighboring cardiomyocytes (24), and comparison of the Cx43 signal-forming links between cardiomyocytes showed significant mislocalization of staining in R735X mutant hearts compared with control subjects expressing *PKP2* or *Luc* only after 8 weeks of swimming exercise (**Figure 5B**). Exercised mutant mice showed abnormal organization at the intercalated disk, with the continuous organization pattern of Cx43 replaced by a punctate distribution. Immunofluorescence analysis of Cx43 organization in 6-month-old sedentary

FIGURE 4 Desmosomal Analysis of Transduced AAV Mice

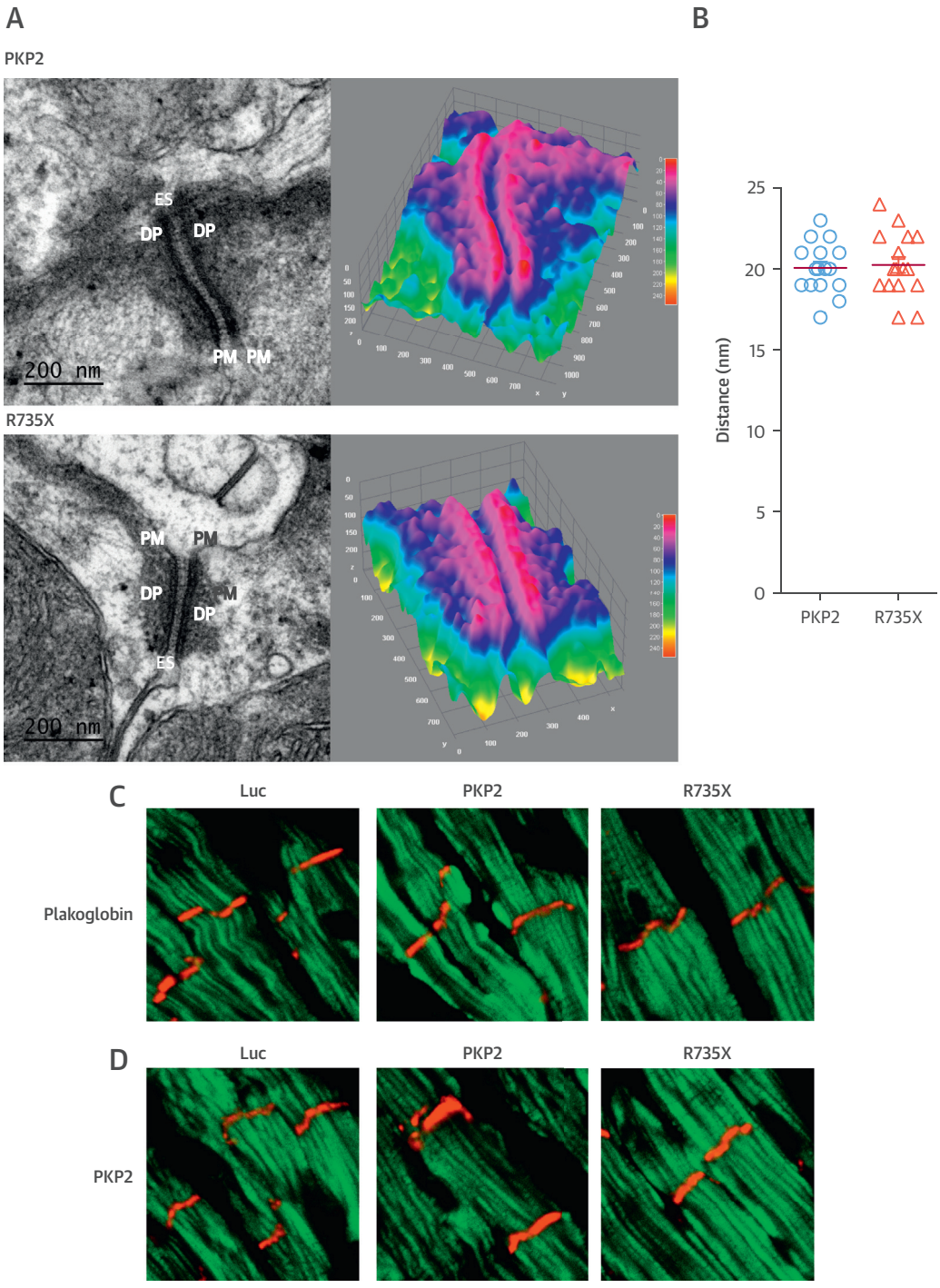

(A) Representative transmission electron microscopy images show intercardiomyocyte desmosome organization in PKP2a- and R735X-transduced heart (DP = dense plaque; ES = extracellular space; PM = plasma membrane). Heat map color code conversions of these images are shown on the right to aid visualization. **(B)** Distance between desmosomal dense plaques in intercardiomyocyte contacts after 8 weeks of endurance training. **(C)** Confocal immunofluorescence of AAV-transduced hearts showing plakoglobin and **(D)** plakophilin-2 localization at the intercalated discs. Cardiomyocyte autofluorescence was used to detect cell limits. Abbreviations as in Figure 1.

FIGURE 5 Local Distribution of Cx43 in Cardiomyocytes From AAV-Injected Animals

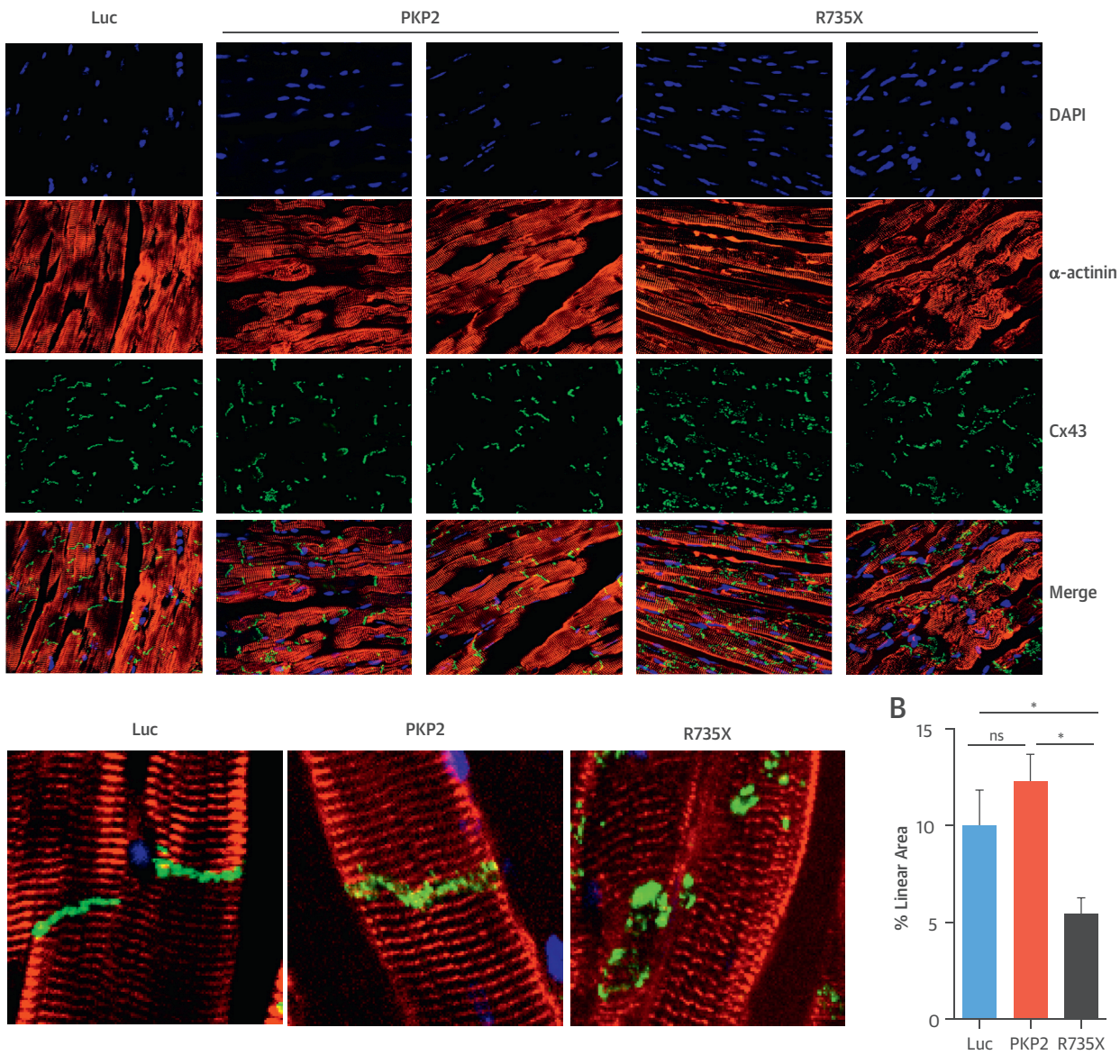

(A) Confocal immunofluorescence of AAV-transduced hearts showing connexin 43 (Cx43) and alpha-actinin localization. The stain 4′,6-diamidino-2-phenylindole (DAPI) was used to detect cell nuclei. **(B)** Mean area of linear Cx43 localization at the edges of cardiomyocytes, in at least 3 animals and >150 cells per transduced gene; *$p < 0.05$. Other abbreviations as in Figure 1.

R735X-infected mice revealed normal localization of Cx43 between cardiomyocytes, which indicates that exercise triggers ARVC in these mice.

DISCUSSION

ARVC is a genetic disease associated with a high risk of heart dysfunction and sudden death. Because the development and progression of heart manifestations in ARVC mutation carriers are difficult to predict, novel research approaches are needed to better study the gene-environment interaction associated with different causal mutations. In this study, we used a novel approach to study the impact of exercise on phenotypic ARVC expression in wild-type mice in which a human *PKP2* mutation was introduced

selectively in the heart by use of AAV vectors. The main results were as follows: 1) A single injection of AAV9 carrying the R735X mutation into wild-type mice results in stable, homogeneous, and long-term expression of the transgene in cardiomyocytes; 2) R735X mutant protein operates as a dominant-negative protein to induce ARVC independent of the expression of the wild-type Pkp2; and 3) although the AAV-mediated R735X mutation expression does not produce an overt ARVC phenotype in sedentary mice, exercise training triggers an ARVC phenotype evidenced by RV regional and global dysfunction, as well as mislocalization of cardiomyocyte Cx43 at the histological level (**Central Illustration**).

Our alternative approach, used here for the first time to study a cardiomyopathy, can boost the evaluation of different mutations and their interaction with the environment and even with other mutations. Our AAV-R735X model could serve to test genetic interactions in combination with new transgenic or knockout models without the need for tedious, costly, and time-consuming backcrosses.

We reasoned that because ventricular dysfunction in ARVC appears after birth and not during development in genetically predisposed patients, expression of disease-causing mutations in adult mouse hearts would trigger development of an ARVC-like phenotype. Our results confirmed this, showing that AAV-based transfer of the R735X dominant-negative form of human *PKP2a* interferes with the wild-type version encoded by the mouse genome and recapitulates the exercise-dependent RV dysfunction of ARVC.

Patients with ARVC frequently show a predominant RV dysfunction without left ventricular (LV) involvement, although the reason behind this remains elusive. However, the ARVC phenotype can vary depending on the desmosomal component affected by the primary mutation. For example, disruption of intermediate filament binding (desmoplakin mutants) can result in dominant or severe LV involvement (8). In contrast, the phenotype associated with PKP2 mutations is that of classic ARVC, which accounts for most cases (25,26). Factors that might make the RV particularly vulnerable to impaired cell adhesion include thin walls, high distensibility, and variations in preload. Indeed, reports have documented reductions in RV function with exercise intensity (15). A link between long-term intensive exercise training, ventricular dysfunction, and predisposition to arrhythmogenic events has also been demonstrated (25,27). Moreover, RV dysfunction can become permanent in some athletes with a long history of competitive sports (28). RV afterload and pulmonary vascular resistance, which is low at rest, may possibly induce an increase in pulmonary artery pressure during training (17). Unlike the transitional or, more rarely, permanent RV dysfunction in endurance athletes, the RV dysfunction associated with ARVC is progressive. In ARVC patients, training would have a greater impact on the RV than the LV if desmosomal mutations give a mechanical disadvantage to cardiomyocytes. Such a predominant effect on the RV has been shown in endurance-trained mice with heterozygous plakoglobin deficiency, in which exercise accelerated the development of RV dysfunction and arrhythmias (29–31). Similar to our mouse model, heterozygous plakoglobin deficiency in mice did not lead to an increase in fibrosis compared with control subjects. These data indicate that the mechanism by which these animals develop local dyskinesia is different from that induced by collagen deposition.

Endurance training increases the risk of developing RV dysfunction in mice expressing R735X by ~5-fold. The available data support the model of the intercalated disc as a functional unit in which macromolecular complexes interact to maintain synchrony in a cell population. These kinds of interactions have been demonstrated between desmosomes and gap junctions, and evidence that supports a functional link between Cx43 and PKP2 provides a possible explanation for the ARVC phenotype (32). In addition to desmosomes, PKP2 is also detected in other junctional structures (33), and the N-terminal head domain of PKP2 interacts directly with Cx43 (22). Our data confirm this interaction and show that cardiac *trans*-expression of mutant R735X in cardiac tissues can alter the distribution pattern of the associated gap junction protein Cx43. Some ARVC patients with mutations in *PKP2* also show abnormal protein levels or localization of Cx43 at the intercalated disk between cardiomyocytes (34), which is consistent with high conservation of desmosome structure throughout vertebrate evolution.

During exercise, right cardiac chambers undergo continuous preload variations and stretch. These forces can upregulate junction protein expression, as shown for mechanical junction proteins (plakoglobin, desmoplakin, and N-cadherin) and the gap junction protein Cx43 in neonatal rat ventricular myocytes subjected to pulsatile stretch (35). Exercise-related stretch has a stronger effect on the thinner RV free wall than on the LV and becomes pathological in patients with a genetic predisposition to lose cardiac tissue structural integrity. Our study shows that exercised R735X-infected mice, although expressing normal levels of Cx43 mRNA, develop an abnormally altered localization and distribution of the encoded gap-junction protein. This finding supports the view

CENTRAL ILLUSTRATION **Exercise Triggers ARVC Phenotype in Mice**

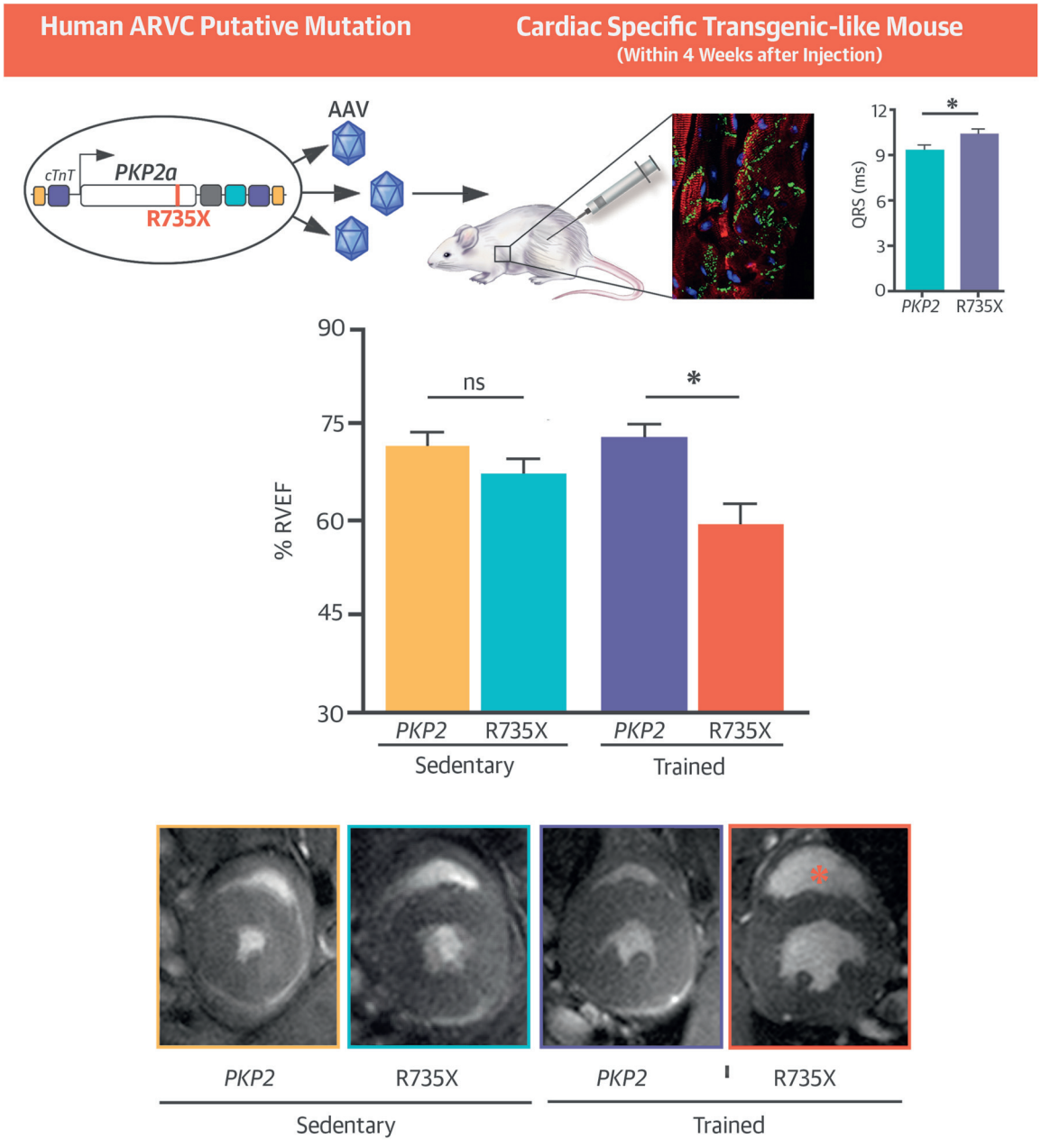

Cruz, F.M. et al. J Am Coll Cardiol. 2015; 65(14):1438–50.

The human arrhythmogenic right ventricular cardiomyopathy (ARVC) mutation of interest is packed within the adeno-associated virus (AAV) vector. The selection of the AAV serotype (AAV9) and the use of the cardiomyocyte-specific troponin T (cTnT) promoter enhance the cardiac-specific infection and expression of the mutant protein. A single injection in wild-type animals (through a peripheral vein) of the AAVs carrying the mutation is enough to generate a transgenic-like mouse. These mice show a stable long-term expression of the mutant protein of interest. The first manifestation of the ARVC phenotype is the widening of the QRS complex. Serial high-field cardiac magnetic resonance (CMR) examinations are performed to evaluate the appearance of ARVC anatomic features. Sedentary mice carrying the ARVC mutation do not show an overt ARVC anatomic phenotype despite showing electrocardiographic abnormalities. Conversely, challenging mice with endurance exercise training results in a clear ARVC anatomic phenotype (areas of right ventricular dyskinesis and global right ventricular ejection fraction [RVEF] reduction). Animals infected with control AAVs undergoing the same exercise protocol do not show any ARVC anatomic features, which suggests that exercise exacerbates the anatomic phenotype of the disease. *Area of dyskinesis.

of the intercalated disc as a functional unit and represents an abnormal response to exercise that triggers multiple pathological changes in the intercellular junction. Junctional changes also impact ion channel activity, with loss of PKP2 expression decreasing the sodium current, which further decreases conduction velocity and makes ventricular myocytes prone to reentrant arrhythmias (36). Therefore, patients in the early stages of ARVC are at risk of lethal cardiac arrhythmia in the absence of structural and histological changes (37).

To better study the phenotype associated with mutant PKP2 expression and its interaction with exercise, surface electrocardiographic recordings were evaluated in trained mice and in long-term sedentary mice. QRS was prolonged in mice expressing the mutant form of PKP2 compared with control subjects, regardless of training status. QRS prolongation is frequently observed in patients with ARVC (38,39), and electrocardiographic abnormalities are an early event in ARVC patients that can precede any anatomic or functional abnormality (40). In that sense, it has been demonstrated that PKP2 and the voltage-gated sodium channel ($Na_V1.5$) coexist in the same molecular complex, and dysfunction of the former alters the properties of the sodium current, which leads to slow conduction velocity (35). Future studies should confirm the association between mutant PKP2 expression and sodium channel properties, something beyond the scope of this work.

Defects in protein trafficking of intercalated discs are crucial for cardiomyocyte injury and development of electrical abnormalities in arrhythmogenic cardiomyopathies (41). We have demonstrated that PKP2 expression of a dominant-negative mutant R735X induces alterations in the localization and distribution of Cx43 at the intercalated discs, a potential origin for disease development. In a *Pkp2* model of haploinsufficiency, cardiomyocytes do not show alteration of proteins at the intercalating disc, although they present a sodium channel dysfunction. These data suggest that the ARVC disease mechanism is different depending on particular mutations in the same gene, which could operate as a dominant-negative protein or haploinsufficiency. Thus, these mechanisms may add variability to the system and to ARVC penetrance.

CLINICAL IMPLICATIONS. The lack of animal models that permit evaluation of different mutations remains a major limitation on research into ARVC. Over the past few years, more than 160 mutations have been described for the *PKP2* gene. It is always important to distinguish disease-causing mutations from normal genetic variability. This is especially important in ARVC, in which gene-carrier patients are advised to radically reduce exercise and withdraw from competitive athletics. The consequences of an erroneous classification are greater for professional athletes, who stand to lose out on their chosen career. Although our data suggest that carriers of the R735X-encoding *PKP2a* mutant (c.2203C>T) should be banned from competitive sport to prevent ARVC development, they also indicate that the exercise-testing platform could be used to distinguish latent disease-causing mutations from nonpathological single-nucleotide polymorphisms.

STUDY LIMITATIONS. In the present study, we only observed early ARVC features (electrocardiogram and wall motion abnormalities), and no fibrofatty ventricular replacement was documented. Longer follow-up of these animals might have revealed additional ARVC features.

CONCLUSIONS

The method described here, with which we showed that the R735X PKP2 mutant functions as a dominant-negative protein in ARVC, provides a versatile platform for investigating this disease. More importantly, we also showed that heterologous expression of wild-type human *PKP2* does not induce disease or altered function, which demonstrates that this approach can be used to evaluate potential disease-causing mutations. Additionally, our methodology represents an unprecedented opportunity to generate complex cardiac disease models and become a powerful tool in preclinical phenotyping and follow-up of complex autosomal-dominant cardiac hereditary disorders.

ACKNOWLEDGEMENTS The authors thank the Centro Nacional de Investigaciones Cardiovasculares Viral Vector Unit for help with adeno-associated virus packaging, A.V. Alonso and M. Benito for heart image acquisition, C. Villa for suggestions on immunofluorescence staining, A. de Molina and R.B. Doohan for tissue sample preparation, K. Sato and A. Sedhukina for help in image analysis, A. Benitez-Sousa for mouse work, A.M. Santos for help with microscopy and ImageJ analysis, D. Filgueiras for critical reading of the manuscript, and S. Bartlett for text editing.

REPRINT REQUESTS AND CORRESPONDENCE: Dr. Juan A. Bernal or Dr. Borja Ibanez, Centro Nacional de Investigaciones Cardiovasculares Carlos III (CNIC), c/Melchor Fernandez Almagro, 3, Madrid 28029, Spain. E-mail: jabernal@cnic.es OR bibanez@cnic.es.

PERSPECTIVES

COMPETENCY IN MEDICAL KNOWLEDGE: Exercise is suspected to trigger clinical events in patients with the genetic mutations associated with ARVC, and animals with the most frequent form of the human R735X *PKP2* mutation subjected to endurance training develop an overt ARVC phenotype.

COMPETENCY IN PATIENT CARE: Experimental data in animals support the recommendation that patients with ARVC who have the R735X *PKP2* mutation curtail the types of exercise associated with endurance training.

TRANSLATIONAL OUTLOOK: Further work using novel methods to study gene-to-gene and gene-environment interactions in transgenic animals could lead to the development of therapeutic strategies that inhibit the adverse effect of sustained exercise on the risk of lethal arrhythmia events and improve health outcomes in patients with ARVC.

REFERENCES

1. Basso C, Corrado D, Marcus FI, Nava A, Thiene G. Arrhythmogenic right ventricular cardiomyopathy. Lancet 2009;373:1289–300.

2. Link MS, Laidlaw D, Polonsky B, et al. Ventricular arrhythmias in the North American multidisciplinary study of ARVC: predictors, characteristics, and treatment. J Am Coll Cardiol 2014;64:119–25.

3. Maron BJ, Chaitman BR, Ackerman MJ, et al. Recommendations for physical activity and recreational sports participation for young patients with genetic cardiovascular diseases. Circulation 2004;109:2807–16.

4. Marcus FI, McKenna WJ, Sherrill D, et al. Diagnosis of arrhythmogenic right ventricular cardiomyopathy/dysplasia: proposed modification of the Task Force Criteria. Eur Heart J 2010;31:806–14.

5. Rizzo S, Pilichou K, Thiene G, Basso C. The changing spectrum of arrhythmogenic (right ventricular) cardiomyopathy. Cell Tissue Res 2012;348:319–23.

6. Marcus FI, Edson S, Towbin JA. Genetics of arrhythmogenic right ventricular cardiomyopathy: a practical guide for physicians. J Am Coll Cardiol 2013;61:1945–8.

7. Groeneweg JA, van der Zwaag PA, Olde Nordkamp LR, et al. Arrhythmogenic right ventricular dysplasia/cardiomyopathy according to revised 2010 Task Force criteria with inclusion of non-desmosomal phospholamban mutation carriers. Am J Cardiol 2013;112:1197–206.

8. van Tintelen JP, Entius MM, Bhuiyan ZA, et al. Plakophilin-2 mutations are the major determinant of familial arrhythmogenic right ventricular dysplasia/cardiomyopathy. Circulation 2006;113:1650–8.

9. Cox MG, van der Zwaag PA, van der Werf C, et al. Arrhythmogenic right ventricular dysplasia/cardiomyopathy: pathogenic desmosome mutations in index-patients predict outcome of family screening: Dutch arrhythmogenic right ventricular dysplasia/cardiomyopathy genotype-phenotype follow-up study. Circulation 2011;123:2690–700.

10. Pilichou K, Bezzina CR, Thiene G, Basso C. Arrhythmogenic cardiomyopathy: transgenic animal models provide novel insights into disease pathobiology. Circ Cardiovasc Genet 2011;4:318–26.

11. Syrris P, Ward D, Asimaki A, et al. Clinical expression of plakophilin-2 mutations in familial arrhythmogenic right ventricular cardiomyopathy. Circulation 2006;113:356–64.

12. Gerull B, Heuser A, Wichter T, et al. Mutations in the desmosomal protein plakophilin-2 are common in arrhythmogenic right ventricular cardiomyopathy [published correction appears in Nat Genet 2005;37:106]. Nat Genet 2004;36:1162–4.

13. Tan BY, Jain R, den Haan AD, et al. Shared desmosome gene findings in early and late onset arrhythmogenic right ventricular dysplasia/cardiomyopathy. J Cardiovasc Transl Res 2010;3:663–73.

14. Prasad KM, Xu Y, Yang Z, Acton ST, French BA. Robust cardiomyocyte-specific gene expression following systemic injection of AAV: in vivo gene delivery follows a Poisson distribution. Gene Ther 2011;18:43–52.

15. James CA, Bhonsale A, Tichnell C, et al. Exercise increases age-related penetrance and arrhythmic risk in arrhythmogenic right ventricular dysplasia/cardiomyopathy-associated desmosomal mutation carriers. J Am Coll Cardiol 2013;62:1290–7.

16. Thiene G, Nava A, Corrado D, Rossi L, Pennelli N. Right ventricular cardiomyopathy and sudden death in young people. N Engl J Med 1988;318:129–33.

17. Kirchhof P, Fabritz L, Zwiener M, et al. Age- and training-dependent development of arrhythmogenic right ventricular cardiomyopathy in heterozygous plakoglobin-deficient mice. Circulation 2006;114:1799–806.

18. Sievers B, Addo M, Franken U, Trappe HJ. Right ventricular wall motion abnormalities found in healthy subjects by cardiovascular magnetic resonance imaging and characterized with a new segmental model. J Cardiovasc Magn Reson 2004;6:601–8.

19. Basso C, Thiene G. Adipositas cordis, fatty infiltration of the right ventricle, and arrhythmogenic right ventricular cardiomyopathy: just a matter of fat? Cardiovasc Pathol 2005;14:37–41.

20. Delmar M, McKenna WJ. The cardiac desmosome and arrhythmogenic cardiomyopathies: from gene to disease. Circ Res 2010;107:700–14.

21. Basso C, Czarnowska E, Della Barbera M, et al. Ultrastructural evidence of intercalated disc remodelling in arrhythmogenic right ventricular cardiomyopathy: an electron microscopy investigation on endomyocardial biopsies. Eur Heart J 2006;27:1847–54.

22. Asimaki A, Tandri H, Huang H, et al. A new diagnostic test for arrhythmogenic right ventricular cardiomyopathy. N Engl J Med 2009;360:1075–84.

23. Palatinus JA, Rhett JM, Gourdie RG. The connexin43 carboxyl terminus and cardiac gap junction organization. Biochim Biophys Acta 2012;1818:1831–43.

24. Jansen JA, van Veen TA, de Bakker JM, van Rijen HV. Cardiac connexins and impulse propagation. J Mol Cell Cardiol 2010;48:76–82.

25. La Gerche A, Burns AT, Mooney DJ, et al. Exercise-induced right ventricular dysfunction and structural remodelling in endurance athletes. Eur Heart J 2012;33:998–1006.

26. Davila-Roman VG, Guest TM, Tuteur PG, Rowe WJ, Ladenson JH, Jaffe AS. Transient right but not left ventricular dysfunction after strenuous exercise at high altitude. J Am Coll Cardiol 1997;30:468–73.

27. Benito B, Gay-Jordi G, Serrano-Mollar A, et al. Cardiac arrhythmogenic remodeling in a rat model of long-term intensive exercise training. Circulation 2011;123:13–22.

28. La Gerche A, Heidbuchel H, Burns AT, et al. Disproportionate exercise load and remodeling of the athlete's right ventricle. Med Sci Sports Exerc 2011;43:974–81.

29. Delmar M, Makita N. Cardiac connexins, mutations and arrhythmias. Curr Opin Cardiol 2012;27:236–41.

30. Noorman M, Hakim S, Kessler E, et al. Remodeling of the cardiac sodium channel, connexin43, and plakoglobin at the intercalated disk in patients with arrhythmogenic cardiomyopathy. Heart Rhythm 2013;10:412–9.

31. Paul M, Wichter T, Gerss J, et al. Connexin expression patterns in arrhythmogenic right ventricular cardiomyopathy. Am J Cardiol 2013;111:1488–95.

32. Sato PY, Coombs W, Lin X, et al. Interactions between ankyrin-G, Plakophilin-2, and Connexin43 at the cardiac intercalated disc. Circ Res 2011;109:193–201.

33. Agullo-Pascual E, Reid DA, Keegan S, et al. Super-resolution fluorescence microscopy of the cardiac connexome reveals plakophilin-2 inside the connexin43 plaque. Cardiovasc Res 2013;100:231–40.

34. Yamada K, Green KG, Samarel AM, Saffitz JE. Distinct pathways regulate expression of cardiac electrical and mechanical junction proteins in response to stretch. Circ Res 2005;97:346–53.

35. Sato PY, Musa H, Coombs W, et al. Loss of plakophilin-2 expression leads to decreased sodium current and slower conduction velocity in cultured cardiac myocytes. Circ Res 2009;105:523–6.

36. Kaplan SR, Gard JJ, Protonotarios N, et al. Remodeling of myocyte gap junctions in arrhythmogenic right ventricular cardiomyopathy due to a deletion in plakoglobin (Naxos disease). Heart Rhythm 2004;1:3–11.

37. Cox MG, Nelen MR, Wilde AA, et al. Activation delay and VT parameters in arrhythmogenic right ventricular dysplasia/cardiomyopathy: toward improvement of diagnostic ECG criteria. J Cardiovasc Electrophysiol 2008;19:775–81.

38. te Riele AS, Bhonsale A, James CA, et al. Incremental value of cardiac magnetic resonance imaging in arrhythmic risk stratification of arrhythmogenic right ventricular dysplasia/cardiomyopathy-associated desmosomal mutation carriers. J Am Coll Cardiol 2013;62:1761–9.

39. te Riele AS, James CA, Rastegar N, et al. Yield of serial evaluation in at-risk family members of patients with ARVD/C. J Am Coll Cardiol 2014;64:293–301.

40. Asimaki A, Kapoor S, Plovie E, et al. Identification of a new modulator of the intercalated disc in a zebrafish model of arrhythmogenic cardiomyopathy. Sci Transl Med 2014;6:240ra74.

41. Cerrone M, Noorman M, Lin X, et al. Sodium current deficit and arrhythmogenesis in a murine model of plakophilin-2 haploinsufficiency. Cardiovasc Res 2012;95:460–8.

KEY WORDS arrhythmia, ARVC, dysplasia, mutation, transgenic mice

APPENDIX For expanded Methods and Results sections, including supplemental videos and their legends, please see the online version of this article.